Published in final edited form as:
J Neurochem. 2012 October ; 123(1): . doi:10.1111/j.1471-4159.2012.07814.x.

CALCYON, A MAMMALIAN SPECIFIC NEEP21 FAMILY MEMBER, INTERACTS WITH ADAPTOR PROTEIN COMPLEX 3 (AP-3) AND REGULATES TARGETING OF AP-3 CARGOES

Nagendran Muthusamy[1,2,*], **Victor Faundez**[3], and **Clare Bergson**[2]

[1]Graduate Program in Neuroscience, Georgia Health Sciences University, Augusta, GA, 30912

[2]Department of Pharmacology and Toxicology, Georgia Health Sciences University, Augusta, GA, 30912

[3]Department of Cell Biology and Center for Neurodegenerative Diseases, Emory University, Atlanta, GA

Abstract

Calcyon is a neural enriched, single transmembrane protein that interacts with clathrin light chain (CLC) and stimulates clathrin assembly and clathrin mediated endocytosis (CME). A similar property is shared by the heterotetrameric adaptor protein (AP) complexes AP-1, AP-2, and AP-3 which recruit cargoes for insertion into clathrin coated transport vesicles. Here we report that AP medium (μ) subunits interact with a YXXØ-type tyrosine motif located at residues 133–136 in the cytoplasmic domain of calcyon. Site specific mutagenesis of the critical tyrosine and bulky hydrophobic residues tyrosine 133 and methionine 136 preferentially abrogated binding of the ubiquitous and neuronal isoforms of μ3, and also impacted μ1 and μ2 binding but to a lesser degree. The relevance of these interactions was explored *in vivo* using mice harboring null-alleles of calcyon. As seen in the mutagenesis studies, calcyon deletion in mice preferentially altered the subcellular distribution of AP-3 suggesting that calcyon could regulate membrane-bound pools of AP-3 and AP-3 function. To test this hypothesis, we focused on the hilar region of hippocampus, where levels of calcyon, AP-3, and AP-3 cargoes are abundant. We analyzed brain cryosections from control and calcyon null mice for zinc transporter 3 (ZnT3), and phosphatidylinositol-4-kinase type II alpha (PI4KIIα), two well-defined AP-3 cargoes. Confocal microscopy indicated that ZnT3 and PI4KIIα are significantly reduced in the hippocampal mossy fibers of calcyon knock-out brain, a phenotype previously described in AP-3 deficiencies. Altogether, our data suggest that calcyon directly interacts with μ3A and μ3B, and regulates the subcellular distribution of AP-3 and the targeting of AP-3 cargoes.

Introduction

Neuron Enriched Endosomal Protein of 21 kDa (NEEP21) (Entrez Gene Name: neuron-specific gene family member 1; alias, nsg1, p21), and P19 (Entrez Gene Name: neuron-specific gene family member 2; alias, nsg2, p19, p1A75) and calcyon (Entrez Gene Name: neuron-specific gene family member 3; alias, nsg3, Drd1ip, Caly), comprise a family of vertebrate specific endocytic proteins robustly expressed in the central nervous system (CNS). Structurally, the gene family is characterized by a single transmembrane segment,

Address correspondence to: Clare Bergson, Ph.D., Department of Pharmacology and Toxicology, Georgia Health Sciences University, 1459 Laney Walker Blvd, Augusta, GA 30912-2300, tel: 706-721-1926; fax: 706-721-2347, cbergson@georigahealth.edu.
*Current address: Center for Comparative Medicine and Translational Research, College of Veterinary Medicine, North Carolina State University, Raleigh, NC 27607.

flanked by approximately equal-length N- and C- terminal domains (Saberan-Djoneidi et al., 1995, 1998; Muthusamy et al., 2009). The P19 zebrafish ortholog appears to be the extant progenitor of the gene family whereas the calcyon lineage shows evidence for positive selection, and is mammalian specific (Muthusamy et al., 2009).

Functional studies suggest that gene family members play distinct roles in regulating vesicle trafficking of transmembrane cargos. For example, NEEP21 regulates the sorting of endocytosed cargo into either a recycling or degradative pathway (Steiner et al., 2002, 2005; Debaigt et al., 2004). In contrast, calcyon regulates clathrin assembly as well as clathrin mediated endocytosis (CME) of plasma membrane localized cargo (Xiao et al., 2006). The distinct endocytic functions of NEEP21 and calcyon involve a non-overlapping set of protein partners. Whereas NEEP21 binds syntaxin 13, and GRIP1 (Steiner et al., 2002, 2005), calcyon interacts with clathrin light chain (CLC) (Xiao et al., 2006).

Although CLC has been implicated in membrane protein trafficking from the trans-Golgi network (TGN) and endosomes (Deborde et al., 2008; Poupon et al., 2008), it is not known whether calcyon regulates clathrin assembly on membrane compartments other than the plasma membrane. Consistent with this possibility, previous studies indicate that calcyon associates with the clathrin adaptor proteins AP-1, AP-2 and AP-3 which regulate clathrin coated vesicle (CCV) formation on a variety of membrane compartments (Xiao et al., 2006).

AP complexes both recruit clathrin to membranes and select cargo to be transported via CCVs (Kirchhausen, 1999). They also exhibit organelle specific functions ranging from CCV formation at the TGN and endosomes for AP-1, to endocytosis from the plasma membrane for AP-2, to targeting endosomal cargo to lysosomes or lysosomes related organelles like melanosomes for AP-3 (Bonifacino and Traub, 2003; Dell'Angelica, 2009). Various AP isoforms carry out tissue specific functions. For example, in polarized epithelial cells, AP-1B, the epithelial specific isoform of AP-1 is involved in the targeting of CCV cargo to the basolateral plasma membrane (Gan et al., 2002). Similarly in neurons, AP-3 regulates the targeting and recycling of selected synaptic vesicle membrane proteins, a process that when perturbed alters the release of neurotransmitters (Feng et al., 1999; Scheuber et al., 2006; Voglmaier et al., 2006). The targeting of synaptic vesicle membrane proteins is defective in AP-3 deficient nerve terminals (Scheuber et al., 2006; Newell-Litwa et al., 2007, 2009). Among the synaptic vesicle proteins impacted by deletion of AP-3 are the zinc transporter (ZnT3) (Salazar et al., 2004b), vesicular chloride channel 3 (ClC-3) (Salazar et al., 2004a), vesicular glutamate transporter (VGLUT1) (Voglmaier et al., 2006), vesicular GABA transporter (VGAT) (Nakatsu et al., 2004), phosphoinositol 4 kinase II alpha (PI4KIIα) (Salazar et al., 2005) and tetanus neurotoxin-insensitive vesicle associated membrane protein (TI-VAMP) (Scheuber et al., 2006).

AP complexes are hetero-tetramers composed of four different subunit chains: two large subunits (β1 – β4 subunits and either a γ, α, δ or ε subunit), one medium subunit (μ1 – μ4), and one small subunit (σ1 – σ4). The β subunits interact with clathrin heavy chain, while μ subunits recognize sorting signals present in the cytosolic domains of transmembrane cargoes such as YXXΦ type tyrosine-based motifs where Y denotes tyrosine, X, any amino acid and Φ, large bulky hydrophobic residue (Ohno et al., 1998). As cytosolic domain of calcyon contains two YXXΦ type motifs, we designed a series of experiments to test the hypothesis that calcyon directly interacts with AP μ subunits *in vitro* as well as in brain. Our data confirm calcyon as a bona fide interacting partner of AP μ subunits, and indicate that in addition to reduced levels of membrane associated AP-3, expression of AP-3 cargoes like ZnT3 and PI4KIIα is altered in mossy fibers of the hippocampus in calcyon knockout ($Cal^{-/-}$) mice. Altogether these data indicate that calcyon by directly interacting with AP-3 regulates the targeting of AP-3 cargoes.

Experimental procedures

Yeast 2-hybrid (Y2H)

DNA encoding the calcyon C terminus (aa 104 to 217) was subcloned into pGBT9 Y2H bait vector. AP Y2H prey constructs pGADT7 μ1 (aa124-423), pACT2 μ2 (aa 123–435) and pGADT7 μ3A (aa123-418) were generously provided by Dr. Carl Creutz, University of Virginia (Creutz and Snyder, 2005) and pACT2 full length μ3B was a gift of Dr. Juan Bonifacino, National Institutes of Child Health and Human Development/NIH. Competent HF7C yeast cells were prepared and transformed using the 'Yeastmaker^{Tm} yeast transformation system 2' (BD Biosciences Clontech) according to the manufacturer's protocol. HF7C cells were plated onto double drop out (−Leu, −Trp, and +His) plates and incubated at 30°C for 3 to 5 days. Single colonies were subsequently streaked onto double and triple drop out (−Leu, −Trp, and −His) plates, and colony growth at 30°C monitored.

Differential centrifugation and glycerol velocity gradients

Ten frozen WT and Cal$^{-/-}$ (Xiao et al., 2006) brains were pulverized to fine powder using excess liquid nitrogen. 5mL of buffer (150mM NaCl, 10mM HEPES, pH 7.4, 1 mM EGTA, and 0.1mM $MgCl_2$) containing a 'complete protease inhibitor cocktail' tablet (Roche) was added to pulverized powder and the proteins extracted at 4°C. Extracts were further homogenized by 16 up/down strokes with a Potter Elvehjem homogenizer at 4°C and centrifuged at 1000× g to obtain S1 supernatants and P1 pellets. S1 supernatants were subjected to further separation by centrifugation at 27,000× g for 45 min to obtain S2 supernatants and P2 pellets. S2 supernatants were resolved in 5–25% glycerol velocity gradients prepared in intracellular buffer (38 mM potassium aspartate, 38mM potassium glutathione, 38 mM potassium gluconate, 20 mM MOPS-KOH, pH 7.2, 5 mM reduced glutathione, 5 mM sodium carbonate, 2.5 mM magnesium sulfate, and 2 mM EGTA) by centrifugation at 218,000× g for 75 min in a SW55 Beckman Coulter rotor. In the eluted fractions, synaptic vesicle peak was determined by immunobloting using monoclonal antibodies to synaptic vesicle protein 2 (SV2).

Immunohistochemistry

Brains from WT and Cal$^{-/-}$ mice were flash frozen in isopentane (2-methyl butane, Sigma) prechilled in a dry ice/ ethanol bath and stored at −80°C until later use. Brains, one from each genotype blinded, were molded together in a block using frozen sectioning medium. Blocks were cut at −18°C into 25 μm thick coronal sections, captured on superfrost plus slides, and stored in −20°C until processed for immunohistochemistry. On the day of immunostaining, sections were fixed with ice cold 4% paraformaldehyde for 20 min at RT and rinsed using SSC buffer (Fisher) followed by ice cold acetone:methanol (1:1) for 20 minutes at RT and rinsed using 0.05% Tween-20 in SSC buffer (SSC-T). Endogenous peroxidase was quenched using 1% hydrogen peroxide solution for 20 minutes at RT. Following the SSC-T washes the sections were blocked using Avidin/Biotin blocking kit (Zymed) as per the protocol. Sections were then incubated for 30 minutes at RT in 0.5% casein in a buffer containing 0.1M Tris-Cl pH 7.5 and 0.15M NaCl (C-BB), followed by incubation at 4°C with rabbit affinity-purified primary antibodies (ZnT3 and PI4KIIα diluted 1:500 in C-BB) for about 60 hours. After SSC-T washes sections were incubated with biotinylated goat anti-rabbit antibody (Vector Laboratories) diluted 1:600 for an hour at RT. Sections were rinsed with SSC-T and then incubated with avidin-biotin peroxidase complex complex (ABC; Vector Laboratories) for an hour at RT. Following the SSC-T rinses, fluorescein tyramide signal amplification (TSA) system was used for direct fluorescence detection. Vectashield mounting medium with DAPI was used and edges sealed with nail polish and stored at 4°C.

Image acquisition and analysis

Confocal Z stack images were taken on a Zeiss LSM 510 microscope and documented using LSM Meta software with hippocampus and hilus of the dendate gyrus in focus using 5×, 25× or 40× objectives as appropriate. ImageJ software was used for post-acquisition measurement of the fluorescent intensity in the hilus region of the dentate gyrus. Briefly, fluorescent intensities for all the sections (1 μm thick) of the Z stack were obtained within equal sized circles encompassing the hilus of the dentate gyrus. The 'fluorescent intensity' for a given stack was obtained by averaging the fluorescent intensity values of the 10 sections in the stack showing the highest labeling. The graph was derived by normalizing average fluorescent intensity values of AP-3 cargo staining in $Cal^{-/-}$ to those from WT samples aligned in the same rostral-caudal location. Cos-7 cell images were acquired with a 63×/1.4 NA objective. The ImageJ function 'Analyze Particles' was used to assess the sizes of the mCherry-calcyon positive puncta in the WT and A^{133} TEA^{136} cells in background subtracted, thresholded images from the middle of the Z-stack.

Statistics

GraphPad Prism 4 was used for statistical analysis of data. Error bars in the graphs represent standard error of the mean (SEM). Experimental conditions were analyzed by Student's t-test or two-way ANOVA as appropriate, followed by post-hoc tests for multiple comparisons as indicated throughout.

Results

Conservation of two AP binding sites in calcyon

Sequence analysis revealed that calcyon (nsg3) contains two YXXΦ motifs typical of adaptor protein (AP) μ subunit binding sites (Fig. S1A). Both the the YDQF motif encompassing residues 108–111 and the YTEM/L motif spanning residues 133–136 are present in all mammalian calcyon genes (Fig. S1B). However, neither motif is present in the comparable segment of the NEEP21 (nsg1) and P19 (nsg2) proteins (Fig. S1A) (Muthusamy et al., 2009).

Direct Interaction of calcyon and AP μ subunits

We performed yeast 2 hybrid (Y2H) assays to validate the interaction between the calcyon C terminus and the AP subunits by transforming cells with different pairs of bait and prey vectors, using empty vectors as controls (Fig. 1A). Colonies grew on the double drop out histidine-containing media regardless of the combination tested. However, only cells transformed with bait vector containing the calcyon C-terminus and prey vector containing either μ1, μ2, μ3A or μ3B subunits grew on the triple drop out histidine-lacking media. These results suggest that prototrophy on histidine-deficient media relies on direct interaction between calcyon with μ subunits of AP-1, AP-2 and AP-3 (Fig. 1B, C).

Association of calcyon and APs in brain

Further studies indicated that endogenous APs and full-length calcyon physically associate in brain. The association was validated using the Cal^{OE} transgenic mice that express FLAG tagged human calcyon in forebrain (30). Anti-FLAG conjugated beads, but not non-immune IgG beads, precipitated FLAG-hCalcyon from Cal^{OE} brain homogenates (Fig. 1D) (Supporting Information). Probing the blots with monoclonal antibodies to the γ subunit of AP-1, α subunit of AP-2, and δ subunit of AP-3 indicated that each of these proteins co-precipitated with FLAG-hCalcyon. The lack of AP bands in the eluates from the non-immune IgG bound beads demonstrated that the co-precipitation was selective. Re-probing the blots with antibodies against 90 kDa heat shock protein (Hsp90) further indicated the

specificity of the AP co-precipitation as Hsp90 was detected only in the input lane (Fig. 1D). These data confirm that calcyon and these APs can be isolated as protein complexes from brain membrane fractions.

To test whether the cytosolic domain of calcyon was sufficient to bind these complexes, we conducted glutathione S transferase (GST) pull-down studies with a GST fusion protein containing the calcyon C-terminus (GST-Cal 104–217) and wild type (WT) brain homogenates as the source of native adaptors (Fig. 1E). GST fused to the cytosolic domain of calcyon selectively retained the γ subunit of AP-1, α subunit of AP-2, and δ subunit of AP-3 on the glutatione resin whereas GST only did not. These results further supported the hypothesis that sequences within the calcyon cytosolic C-terminus are sufficient for interaction with endogenous AP's.

To test whether the association involved direct binding of AP μ subunits, we used the GST fusion proteins described above as well as purified, recombinant AP μ subunits expressed *in vitro* as S-tag fusion proteins. These studies revealed a robust ability of immobilized GST-Cal 104–217, but not GST only, to retain all of the S-μ fusion proteins (Fig. 1F, G). The results suggested that the co-precipitation of native AP's from brain is mediated by direct interaction of the calcyon C-terminus and AP μ subunits.

The first 'YXXΦ' motif is not required for binding

AP μ subunits exhibit sequence-dependent differences in their affinity for YXXΦ motifs (Ohno et al., 1998). As shown in Fig. S1, there are two canonical AP binding motifs in the calcyon C terminus (Tm-KAIWYDQF-20aa-YYTEM-81aa). We pinpointed the region in calcyon important for AP binding using the S-tagged μ fusion proteins described above, and a set of GST fusion proteins containing serial truncations from the N-terminus of the calcyon cytosolic domain (Fig. S2A) (Supporting Information). Fusion proteins containing either full-length calcyon C-terminus or a version with the first YXXΦ motif deleted (i.e., GST-Cal 114–217 and GST-Cal 104–217) bound equivalent levels of the μ subunits. These findings indicated that juxta- transmembrane domain residues 104 to 113 including the first YXXΦ motif in calcyon do not play a major role in AP interaction. This was confirmed by mutagenesis of the first tyrosine motif in the context of the entire calcyon C terminus. Neither single (A^{108}DQF or YDQA^{111}) nor the double (A^{108}DQA^{111}) amino acid substitution impacted binding (Fig. S2B, C). In contrast, deletion of residues 104 to 136 encompassing the second YXXΦ motif significantly impaired the binding of all μ subunits relative to levels bound to GST-Cal 104–217 ($p<0.05$, for μ2, and μ3B; <0.01 for μ1, and μ3A). Furthermore, there was no detectable binding of AP μ subunits to the calcyon C-terminus containing only residues found distal to the second YXXΦ motif (GST-Cal 155–217, Fig S2). Collectively, these data indicate that while the first YXXΦ motif is dispensable for μ subunit binding, calcyon binding involves residues in or proximal to the second tyrosine-based motif.

Mutation of the second 'YXXΦ' motif disrupts μ binding

Interactions between YXXΦ-based motifs and μ subunits are critically dependent on the tyrosine and the bulky hydrophic residues of the sorting signal (Owen and Evans, 1998; Creutz and Snyder, 2005). We addressed whether the second tyrosine-based motif (Y^{133}TEM^{136}) in calcyon conformed to this critical property in pull down experiments of recombinant μ subunits with GST-Cal 104–217 harboring mutations in this motif (A^{133}TEA^{136}, Fig. 2A). The A^{133}TEA^{136} mutant significantly lowered the binding of all AP μ subunits compared to levels bound to wild type GST-Cal 104–217 ($p<0.01$ to 0.001, two way ANOVA, Bonferroni post-test) (Fig. 2B, C). Residual binding of μ1 and μ2 to the A^{133}TEA^{136} calcyon mutant ranged between ~40 to ~50% of wild type levels. However,

this binding activity was above of that observed for GST only ($p<0.05$, two-way ANOVA, $A^{133}TEA^{136}$ vs GST only). In contrast, recombinant S-tagged μ3A and S-tagged μ3B binding to the calcyon double mutant was reduced to background levels observed with GST only ($p>0.05$ for both, two-way ANOVA, $A^{133}TEA^{136}$ vs GST only). These data suggest that the YTEM motif as well as additional sequences in calcyon mediate interaction with the μ1 and μ2 subunits. In contrast, the findings are consistent with a model in which the second tyrosine motif in the calcyon cytoplasmic tail is the sole determinant for interaction with μ3A and μ3B.

Fluorescent confocal microscopy studies revealed that the $A^{133}TEA^{136}$ mutation in the context of full-length protein altered the subcellular localization of calcyon (Fig. 2D,E). When expressed as mCherry fusion proteins in Cos-7 cells, both the calcyon WT and mutant proteins exhibit a punctate distribution throughout the cytoplasm indicating enrichment in vesicles. However, there were significant differences in both the overall distribution as well as the size of the mCherryCalcyon-WT and $A^{133}TEA^{136}$ puncta. WT calcyon positive vesicles were significantly larger (n=792 puncta, 6 cells) than the $A^{133}TEA^{136}$ vesicles (n=744 puncta, 6 cells) (895.3+/−44.88 nm^2 versus 756.9+/−31.36 nm^2) ($p<0.05$, unpaired t-test). In addition, the mCherryCalcyon-WT vesicles were distributed in the cytoplasm in a radial gradient with peak levels in a perinuclear compartment. In contrast, the mCherryCalcyon-ATEA vesicles showed a more dispersed distribution, and were not concentrated in any particular region of the cytoplasm.

Deletion of calcyon leads to differential distribution of AP complexes

The presence of a tyrosine motif in calcyon capable of binding μ subunits suggests that calcyon could act as a passive cargo loaded into vesicles. This hypothesis contrasts with our previous observations that calcyon regulates clathrin assembly as well as CME, a function reminiscent of the roles of APs. These observations suggest that calcyon could act as a regulator of adaptor function by its interactions with these complexes. This hypothesis predicts that loss-of-function alleles of calcyon would perturb AP subcellular distribution as well as the targeting of AP cargoes. In contrast, if calcyon acts as a passive cargo for adaptors, neither adaptor distribution, nor cargo sorting should be altered in calcyon null mutants.

To discriminate between these hypotheses, we performed subcellular fractionation of WT and $Cal^{-/-}$ brains to determine whether deletion of calcyon impacts AP membrane distribution. Synaptic vesicle (SV)-containing high-speed supernatants (S2) were separated from larger membranes (P1 and P2) by differential centrifugation. The P1, P2 and S2 fractions were subjected to SDS PAGE, and subsequently immunoblotted with antibodies to the γ, α, and δ subunits. Normalizing AP to GAPDH levels indicated that levels of AP-3δ were elevated in the $Cal^{-/-}$ S2 fractions compared to levels in WT samples (*, $p< 0.05$; t-test) (Fig. 3A, B). Levels of AP-3 were also significantly lower in the $Cal^{-/-}$ P2 fraction compared to WT ($p<0.01$ two-way ANOVA, Bonferroni post-test) (Fig. 3D, C). Importantly, the reduction in AP-3 in P2 fractions correlated with increased levels detected in the S2 fraction. In contrast, equivalent levels of AP-1 and AP-2 were detected in WT and $Cal^{-/-}$ S2 and P2 fractions. Deletion of calcyon also did not impact levels of adaptor proteins in the P1 fraction.

We next asked whether deletion of calcyon altered AP-mediated targeting of SV membrane proteins by subjecting S2 supernatants to glycerol gradient velocity sedimentation. Fractions were immunoblotted and SV enriched fractions identified by probing with antibodies to synaptic vesicle protein 2 (SV2) (Fig. S3). The SV marker was detected in gradient fractions 1 to 9, with higher levels in fractions 4 to 6. Importantly, the sedimentation profile for SV2

did not differ in the WT and Cal$^{-/-}$ gradients, suggesting that deletion of the calcyon gene does not result in global alterations in SV protein fractionation.

AP distribution in the glycerol gradient fractions was determined by re-probing the blots with antibodies to the γ, α, and δ subunits (Fig. 4A). AP-2 was detected in all fractions. In contrast, AP-1 and AP-3 were enriched in SV2 negative fractions containing the cytosolic marker β-actin, and sedimented in a symmetric peak centered on fraction 11 (Fig. 4A, B). Notably, AP-1 and AP-3 were significantly more abundant in the Cal$^{-/-}$ fractions (fraction 9, $p<0.05$ for AP-1; fraction 10, $p<0.01$ for AP-1 and AP-3; fraction 11, $p<0.05$ and $p<0.001$ for AP-1 and AP-3, respectively; and fraction 12, $p<0.001$ for AP-3; two-way ANOVA, Bonferroni post-test) (Fig. 4B). However, the differences were less dramatic for AP-1, and could account for the equivalent levels of the γ subunit detected in WT and Cal$^{-/-}$ P2 fractions. While a similar trend was observed for AP-2 in fractions 10 to 12, the differences did not reach significance. Equivalent levels of the cytoskeletal protein β-actin were also detected in these fractions of the WT and Cal−/− gradients (Fig. 4B). Together, the reciprocal alterations in AP-3 levels in the Cal$^{-/-}$ S2 and P2 fractions (Fig. 3), and the almost fivefold increase in the levels of AP-3 observed in Cal−/− gradient fractions (Fig. 4), suggest the deletion of the calcyon gene would have pronounced impact on the subcellular distribution of AP-3 in brain.

Calcyon regulates trafficking of AP-3 cargoes to hippocampal mossy fibers

AP-3 regulates divergent movement of cargo from sorting endosomes along pathways leading to synaptic vesicles (neuron specific) or to lysosomes and lysosome-related organelles (ubiquitous). In neurons, AP-3 is involved in the targeting of specific SV membrane proteins to axon terminals. For example, zinc transporter 3 (ZnT3) is mis-localized in mice in which the AP-3δ gene is deleted (mocha mice) (Salazar et al., 2004b). As our data suggest mis-localization of AP-3 in Cal$^{-/-}$ mice, they predict that targeting of AP-3 cargoes could be affected by calcyon deficiency. To this end, we analyzed the distribution and content of ZnT3 in glycerol gradient fractions of the S2 high-speed supernatants (Fig. 5A). However, the sedimentation profile of ZnT3 in the Cal$^{-/-}$ fractions closely matched that observed in the WT fractions (Fig. 5B).

AP-3 is prominently expressed in the hilus and CA3 region of hippocampus where the effects of AP-3δ gene deletion on SV cargo targeting in the mossy fiber tract are robust (Salazar et al., 2004a, 2004b; Scheuber et al., 2006). Calcyon is also enriched in CA3 and dentate gyrus (Zelenin et al., 2002; Oakman and Meador-Woodruff, 2004). Therefore, we hypothesized that ZnT3 levels would be altered in Cal$^{-/-}$ mossy fibers in the hilus of the dentate gyrus. To test this, ZnT3 was localized in hippocampal sections of WT and Cal$^{-/-}$ mice (n=3) by fluorescent immunohistochemistry (Fig. 5C,D). Comparison of ZnT3 labeling intensity in the hilus indicated lower levels in the Cal$^{-/-}$ sections ($p<0.01$, t-test) (Fig. 5E). ZnT3 is preferentially sorted to neuronal processes and synaptic vesicles, and is abundant in neuron terminals (Seong et al., 2005). Therefore, we also compared levels of the ZnT3 in the axons of the hilus and terminals of the mossy fiber projections in sections from WT and Cal$^{-/-}$ mice. ZnT3 antibodies labeled the entire axonal projection as well as in mossy fiber terminals of both the control and knockout brains. However, the staining intensity of the terminals in the CA3 region relative to that of the axons in the hilus was lower in the Cal$^{-/-}$ sections ($p<0.05$, t-test) (Fig. 5F, G). These data suggest impaired targeting of ZnT3 to mossy fiber terminals in the absence of calcyon.

Like ZnT3, phosphoinositol 4-kinase type II alpha (PI4KIIα) is an AP-3 cargo that is also abundant in MF projection (Craige et al., 2008). As observed for ZnT3, deletion of calcyon impacted neither the levels nor distribution of PI4KIIα in the glycerol gradient (Fig. 6A,B). However, immunostaining revealed reduced levels of PI4KIIα in the hilus of the Cal$^{-/-}$

compared to WT ($p<0.05$, t-test) (Fig. 6C–E). Interestingly, in the absence of AP-3 complexes (*mocha*), the kinase redistributes to the perinuclear Golgi area (Salazar et al., 2005; Larimore et al., 2011). If calcyon regulates AP-3 distribution in the MF tract, we predicted that subcellular distribution of PI4KIIα in granule cells in the dentate gyrus should be altered as the result of calcyon gene deletion. We compared levels of PI4KIIα staining in granule cell bodies and axons in the adjacent region of the hilus. This analysis showed that relative levels of cell body staining are stronger, and axonal staining lower in $Cal^{-/-}$ compared to WT samples ($p<0.05$, t-test) (Fig. 6F, G). Altogether, these data on the ZnT3 and PI4KIIα point to a role for calcyon in regulating AP-3 cargo targeting in mossy fibers.

Discussion

The findings of the present study validate that calcyon directly interacts with μ subunits of the AP complexes AP-1, AP-2, and AP-3, and preferentially, but not exclusively regulates the subcellular distribution of AP-3 and the targeting of AP-3 cargoes. At least four lines of evidence support these conclusions. First, deletion or mutation of the critical tyrosine and bulky hydrophobic residue in the second YXXΦ type tyrosine motif of calcyon significantly reduced binding of all AP μ subunits studied. Second, double alanine point mutations ($A^{133}TEA^{136}$) impacted μ3A and μ3B subunit binding to a greater extent than μ1 and μ2 binding. Third, significantly reduced levels of AP-3 are observed in the high-speed membrane pellet (P2 fraction) of $Cal^{-/-}$ brain, along with a corresponding increase in AP-3 levels in the cytosolic, SV2 negative glycerol gradient fractions. Additionally, levels of two AP-3 cargoes, ZnT3 and PI4KIIα are significantly reduced in the mossy fibers of $Cal^{-/-}$ hippocampus. Altogether the above data indicates that calcyon regulates targeting of AP-3 cargoes by directly interacting with μ3A and μ3B.

The binding of calcyon to all AP μ subunits tested is consistent with the overlapping sequence specificity of μ1, μ2, μ3A, and μ3B for residues in and around the YXXΦ motif (Ohno et al., 1998). While μ2 subunits recognize the broadest range of sequence variants, the binding of μ3A and μ3B subunits correlates well with the presence of glutamic acid residues before and after the critical tyrosine reside as seen in the EMY**Y**TEM motif (critical tyrosine in bold) in calcyon (Ohno et al., 1998; Bonifacino and Traub, 2003). Indeed, the binding of both μ3 isoforms to calcyon strongly depended on the YXXΦ motif in this sequence context as the $A^{133}TEA^{136}$ mutant altogether eliminated binding of μ3A and μ3B to calcyon. In contrast, approximately half of μ1 and μ2 binding activity was resistant to the $A^{133}TEA^{136}$ mutation, indicating that sequences distinct from this motif also contribute to the binding of these μ subunits. Based on the relative selectivity of μ3A and μ3B for the calcyon YXXΦ motif, it is tempting to speculate that calcyon preferentially interacts with AP-3 *in vivo* as suggested by the hippocampal phenotypes in calcyon null brains.

Phosphoinositide phospholipids, ARF-GTPases, and sorting signals in transmembrane cargoes are among the factors known to regulate AP membrane recruitment (Ooi et al., 1998; Baust et al., 2008). Here, whole brain membrane protein fractionation studies indicate that calcyon also plays a role in AP membrane recruitment. Specifically, $Cal^{-/-}$ brains exhibit elevated levels of AP-1 and AP-3 in cytosolic fractions, and significantly reduced levels of membrane-associated AP-3. These alterations in AP subcellular distribution detected in the calcyon null brains point to impaired membrane recruitment in the absence of calcyon. As calcyon binds to AP μ subunits, the current data are consistent with a model where calcyon uses the YXXΦ motif typically found in cargo proteins to influence AP-1, and especially AP-3 membrane recruitment.

The apparent subunit selectivity in AP membrane recruitment corresponds closely with the subcellular distribution of calcyon. Calcyon is enriched in vesicular compartments

associated with AP-1 and AP-3 functions including endosomes, TGN and lysosomes (Bonifacino and Traub, 2003; Xiao et al., 2006). In contrast, low levels (less than 10% of the total pool) are present on the cell surface where AP-2 stimulates clathrin-mediated endocytosis (Ali and Bergson, 2003). While calcyon might be an AP-2 cargo, an alternate possibility is that calcyon regulates AP-2 membrane association in an activity-dependent fashion such as is the case in the regulation of α-amino-3-hydroxy-5-methyl-4-isoxazoleproprionic acid (AMPA) glutamate receptor endocytosis (Davidson et al., 2009). Deletion of calcyon significantly impairs synaptic activity-dependent internalization of AMPA receptors, whereas constitutive, activity-independent AMPA receptor endocytosis is unaffected by the calcyon null alleles (Luscher et al., 1999; Davidson et al., 2009). Additionally, increases in intracellular calcium levels, as occurs during synaptic activity, trigger translocation of calcyon to the plasma membrane, would be predicted to enhance the possibility of interaction with AP-2 (Ali and Bergson, 2003).

A predicted consequence of altered recruitment of APs to membranes would be the mis-sorting of cargoes. In particular, as calcyon interacts with both the ubiquitous and neuronal μ3 subunits, the alterations could include endosomal sorting to the lysosomal, lysosomal related organelle, and/or SV pathways. A number of studies indicate that the mossy fiber projection in the hilus of the dentate gyrus is useful system for elucidating AP-3 dependent functions in brain (Salazar et al., 2004a, 2004b; Seong et al., 2005; Scheuber et al., 2006; Newell-Litwa et al., 2007, 2010) (Larimore et al., 2011). Levels of both of the AP-3 cargoes tested here, ZnT3 and PI4KIIα, are significantly reduced in mossy fibers of the $Cal^{-/-}$ brains. In addition, relative levels of ZnT3 in CA3 are lower in $Cal^{-/-}$ brains, and relative levels of PI4KIIα in granule cell axons in the hilus are also reduced. While both phenotypes (lower levels and mis-localization) are indicative of targeting defects, the gradient sedimentation profiles of these AP-3 cargoes conducted with whole brain homogenates suggested that the subcellular distribution of ZnT3 and PI4KIIα are unaltered by deletion of calcyon. There are several possible explanations for the apparent discrepancy in the whole brain homogenate and mossy fiber data. Notably, compared to expression levels in other brain regions, both calcyon and AP-3 are enriched in the mossy fiber projection of granule cells in the dentate gyrus to the CA3 region of hippocampus (Zelenin et al., 2002; Oakman and Meador-Woodruff, 2004; Scheuber et al., 2006). However, predicting the consequences of calcyon gene deletion on AP-3 cargo distribution in mossy fibers is complicated by the fact that AP-3 has two sites of action, the cell body and nerve terminal (Larimore et al., 2011). The alterations in ZnT3 and PI4KIIα detected could indicate that calcyon influences both mechanisms. This possibility is consistent with the known enrichment of calcyon in cell bodies and nerve terminals (Xiao et al., 2006). As mentioned above, aside from calcyon described in this study, a number of other factors are known to play a role in AP-3 membrane recruitment. The expression of these factors, or an excess of AP-3 relative to that of calcyon levels in the dentate gyrus could mitigate the relative impact of deleting calcyon on AP-3 cargo trafficking. In addition, mossy fiber terminals in CA3 are elaborated in ways atypical of most synaptic boutons in the CNS, including an unusually large number of active zones per terminal (upwards of thirty) (Chicurel and Harris, 1992; Acsády et al., 1998) as well as size of the synaptic vesicle pool (Suyama et al., 2007). Therefore, the mossy fiber axon terminals themselves display a number of fortuitous features that may underlie the prominent region specific effects detected in the $Cal^{-/-}$ brains.

The present studies highlight a new role for calcyon in AP-3 recruitment to membranes and the targeting of AP-3 cargoes in mossy fibers, whereas previous work demonstrated that calcyon is required for NMDA-dependent long term synaptic depression, a form of synaptic plasticity requiring AMPA receptor endocytosis (Davidson et al., 2009). The interaction of calcyon with two proteins associated with CCV assembly: clathrin light chain and AP μ subunits, presumably accounts for at least in the cargo trafficking and receptor endocytosis

deficits detected in $Cal^{-/-}$ brain. Indeed, the second tyrosine motif shown here to be important for μ subunit binding is also positioned in the CLC binding domain of calcyon (residues 123 to 155) (Fig. S1) (Davidson et al., 2009). As such, it appears that calcyon functions as transmembrane adaptor protein scaffold which facilitates vesicle trafficking to axonal boutons as well as away from dendritic synapses. Finally, our studies suggest that like the closely related protein NEEP21 (Yap et al., 2008), calcyon regulates the sorting of both axonal and somatodendritic cargoes (Davidson et al., 2009).

Supplementary Material

Refer to Web version on PubMed Central for supplementary material.

References

Acsády L, Kamondi A, Sík A, Freund T, Buzsáki G. GABAergic cells are the major postsynaptic targets of mossy fibers in the rat hippocampus. J. Neurosci. 1998; 18:3386–3403. [PubMed: 9547246]

Ali MK, Bergson C. Elevated intracellular calcium triggers recruitment of the receptor cross-talk accessory protein calcyon to the plasma membrane. J.Biol.Chem. 2003; 278:51654–51663. [PubMed: 14534309]

Baust T, Anitei M, Czupalla C, Parshyna I, Bourel L, Thiele C, Krause E, Hoflack B. Protein networks supporting AP-3 function in targeting lysosomal membrane proteins. Mol. Biol. Cell. 2008; 19:1942–1951. [PubMed: 18287518]

Bonifacino JS, Traub LM. Signals for sorting of transmembrane proteins to endosomes and lysosomes. Annu. Rev. Biochem. 2003; 72:395–447. [PubMed: 12651740]

Chicurel ME, Harris KM. Three-dimensional analysis of the structure and composition of CA3 branched dendritic spines and their synaptic relationships with mossy fiber boutons in the rat hippocampus. J. Comp. Neurol. 1992; 325:169–182. [PubMed: 1460112]

Craige B, Salazar G, Faundez V. Phosphatidylinositol-4-kinase type II alpha contains an AP-3-sorting motif and a kinase domain that are both required for endosome traffic. Mol. Biol. Cell. 2008; 19:1415–1426. [PubMed: 18256276]

Creutz CE, Snyder SL. Interactions of annexins with the mu subunits of the clathrin assembly proteins. Biochemistry. 2005; 44:13795–13806. [PubMed: 16229469]

Davidson HT, Xiao J, Dai R, Bergson C. Calcyon is necessary for activity-dependent AMPA receptor internalization and LTD in CA1 neurons of hippocampus. Eur.J.Neurosci. 2009; 29:42–54. [PubMed: 19120439]

Debaigt C, Hirling H, Steiner P, Vincent JP, Mazella J. Crucial role of neuron-enriched endosomal protein of 21 kDa in sorting between degradation and recycling of internalized G-protein-coupled receptors. J.Biol.Chem. 2004; 279:35687–35691. [PubMed: 15187090]

Deborde S, Perret E, Gravotta D, Deora A, Salvarezza S, Schreiner R, Rodriguez-Boulan E. Clathrin is a key regulator of basolateral polarity. Nature. 2008; 452:719–723. [PubMed: 18401403]

Dell'Angelica EC. AP-3-dependent trafficking and disease: the first decade. Curr. Opin. Cell Biol. 2009; 21:552–559. [PubMed: 19497727]

Feng L, Seymour AB, Jiang S, To A, Peden AA, Novak EK, Zhen L, Rusiniak ME, Eicher EM, Robinson MS, et al. The beta3A subunit gene (Ap3b1) of the AP-3 adaptor complex is altered in the mouse hypopigmentation mutant pearl, a model for Hermansky-Pudlak syndrome and night blindness. Hum. Mol. Genet. 1999; 8:323–330. [PubMed: 9931340]

Gan Y, McGraw TE, Rodriguez-Boulan E. The epithelial-specific adaptor AP1B mediates post-endocytic recycling to the basolateral membrane. Nat. Cell Biol. 2002; 4:605–609. [PubMed: 12105417]

Kirchhausen T. Adaptors for clathrin-mediated traffic. Annu. Rev. Cell Dev. Biol. 1999; 15:705–732. [PubMed: 10611976]

Larimore J, Tornieri K, Ryder PV, Gokhale A, Zlatic SA, Craige B, Lee JD, Talbot K, Pare J-F, Smith Y, et al. The schizophrenia susceptibility factor dysbindin and its associated complex sort cargoes from cell bodies to the synapse. Mol. Biol. Cell. 2011; 22:4854–4867. [PubMed: 21998198]

Luscher C, Xia H, Beattie EC, Carroll RC, von Zastrow M, Malenka RC, Nicoll RA. Role of AMPA receptor cycling in synaptic transmission and plasticity. Neuron. 1999; 24:649–658. [PubMed: 10595516]

Muthusamy N, Ahmed SA, Rana BK, Navarre S, Kozlowski DJ, Liberles DA, Bergson C. Phylogenetic analysis of the NEEP21/calcyon/P19 family of endocytic proteins: evidence for functional evolution in the vertebrate CNS. J. Mol. Evol. 2009; 69:319–332. [PubMed: 19760447]

Nakatsu F, Okada M, Mori F, Kumazawa N, Iwasa H, Zhu G, Kasagi Y, Kamiya H, Harada A, Nishimura K, et al. Defective function of GABA-containing synaptic vesicles in mice lacking the AP-3B clathrin adaptor. J.Cell Biol. 2004; 167:293–302. [PubMed: 15492041]

Newell-Litwa K, Chintala S, Jenkins S, Pare J-F, McGaha L, Smith Y, Faundez V. Hermansky-Pudlak protein complexes, AP-3 and BLOC-1, differentially regulate presynaptic composition in the striatum and hippocampus. J. Neurosci. 2010; 30:820–831. [PubMed: 20089890]

Newell-Litwa K, Salazar G, Smith Y, Faundez V. Roles of BLOC-1 and adaptor protein-3 complexes in cargo sorting to synaptic vesicles. Mol. Biol. Cell. 2009; 20:1441–1453. [PubMed: 19144828]

Newell-Litwa K, Seong E, Burmeister M, Faundez V. Neuronal and non-neuronal functions of the AP-3 sorting machinery. J. Cell. Sci. 2007; 120:531–541. [PubMed: 17287392]

Oakman SA, Meador-Woodruff JH. Calcyon transcript expression in macaque brain. J.Comp Neurol. 2004; 468:264–276. [PubMed: 14648684]

Ohno H, Aguilar RC, Yeh D, Taura D, Saito T, Bonifacino JS. The medium subunits of adaptor complexes recognize distinct but overlapping sets of tyrosine-based sorting signals. J. Biol. Chem. 1998; 273:25915–25921. [PubMed: 9748267]

Ooi CE, Dell'Angelica EC, Bonifacino JS. ADP-Ribosylation factor 1 (ARF1) regulates recruitment of the AP-3 adaptor complex to membranes. J. Cell Biol. 1998; 142:391–402. [PubMed: 9679139]

Owen DJ, Evans PR. A structural explanation for the recognition of tyrosine-based endocytotic signals. Science. 1998; 282:1327–1332. [PubMed: 9812899]

Poupon V, Girard M, Legendre-Guillemin V, Thomas S, Bourbonniere L, Philie J, Bright NA, McPherson PS. Clathrin light chains function in mannose phosphate receptor trafficking via regulation of actin assembly. Proc. Natl. Acad. Sci. U.S.A. 2008; 105:168–173. [PubMed: 18165318]

Saberan-Djoneidi D, Marey-Semper I, Picart R, Studler JM, Tougard C, Glowinski J, Levi-Strauss M. A 19-kDa protein belonging to a new family is expressed in the Golgi apparatus of neural cells. J.Biol.Chem. 1995; 270:1888–1893. [PubMed: 7829526]

Saberan-Djoneidi D, Picart R, Escalier D, Gelman M, Barret A, Tougard C, Glowinski J, Levi-Strauss M. A 21-kDa polypeptide belonging to a new family of proteins is expressed in the Golgi apparatus of neural and germ cells. J.Biol.Chem. 1998; 273:3909–3914. [PubMed: 9461575]

Salazar G, Craige B, Wainer BH, Guo J, De Camilli P, Faundez V. Phosphatidylinositol-4-kinase type II alpha is a component of adaptor protein-3-derived vesicles. Mol. Biol. Cell. 2005; 16:3692–3704. [PubMed: 15944223]

Salazar G, Love R, Styers ML, Werner E, Peden A, Rodriguez S, Gearing M, Wainer BH, Faundez V. AP-3-dependent mechanisms control the targeting of a chloride channel (ClC-3) in neuronal and non-neuronal cells. J. Biol. Chem. 2004a; 279:25430–25439. [PubMed: 15073168]

Salazar G, Love R, Werner E, Doucette MM, Cheng S, Levey A, Faundez V. The zinc transporter ZnT3 interacts with AP-3 and it is preferentially targeted to a distinct synaptic vesicle subpopulation. Mol. Biol. Cell. 2004b; 15:575–587. [PubMed: 14657250]

Scheuber A, Rudge R, Danglot L, Raposo G, Binz T, Poncer J-C, Galli T. Loss of AP-3 function affects spontaneous and evoked release at hippocampal mossy fiber synapses. Proc. Natl. Acad. Sci. U.S.A. 2006; 103:16562–16567. [PubMed: 17056716]

Seong E, Wainer BH, Hughes ED, Saunders TL, Burmeister M, Faundez V. Genetic analysis of the neuronal and ubiquitous AP-3 adaptor complexes reveals divergent functions in brain. Mol. Biol. Cell. 2005; 16:128–140. [PubMed: 15537701]

Steiner P, Alberi S, Kulangara K, Yersin A, Sarria JC, Regulier E, Kasas S, Dietler G, Muller D, Catsicas S, et al. Interactions between NEEP21, GRIP1 and GluR2 regulate sorting and recycling of the glutamate receptor subunit GluR2. Embo J. 2005; 24:2873–2884. [PubMed: 16037816]

Steiner P, Sarria JC, Glauser L, Magnin S, Catsicas S, Hirling H. Modulation of receptor cycling by neuron-enriched endosomal protein of 21 kD. J.Cell Biol. 2002; 157:1197–1209. [PubMed: 12070131]

Suyama S, Hikima T, Sakagami H, Ishizuka T, Yawo H. Synaptic vesicle dynamics in the mossy fiber-CA3 presynaptic terminals of mouse hippocampus. Neurosci. Res. 2007; 59:481–490. [PubMed: 17933408]

Trantham-Davidson H, Vazdarjanova A, Dai R, Terry A, Bergson C. Up-regulation of calcyon results in locomotor hyperactivity and reduced anxiety in mice. Behav.Brain Res. 2008; 189:244–249. [PubMed: 18295356]

Voglmaier SM, Kam K, Yang H, Fortin DL, Hua Z, Nicoll RA, Edwards RH. Distinct endocytic pathways control the rate and extent of synaptic vesicle protein recycling. Neuron. 2006; 51:71–84. [PubMed: 16815333]

Xiao J, Dai R, Negyessy L, Bergson C. Calcyon, a novel partner of clathrin light chain, stimulates clathrin-mediated endocytosis. J.Biol.Chem. 2006; 281:15182–15193. [PubMed: 16595675]

Yap CC, Wisco D, Kujala P, Lasiecka ZM, Cannon JT, Chang MC, Hirling H, Klumperman J, Winckler B. The somatodendritic endosomal regulator NEEP21 facilitates axonal targeting of L1/NgCAM. J.Cell Biol. 2008; 180:827–842. [PubMed: 18299352]

Zelenin S, Aperia A, Diaz HR. Calcyon in the rat brain: cloning of cDNA and expression of mRNA. J.Comp Neurol. 2002; 446:37–45. [PubMed: 11920718]

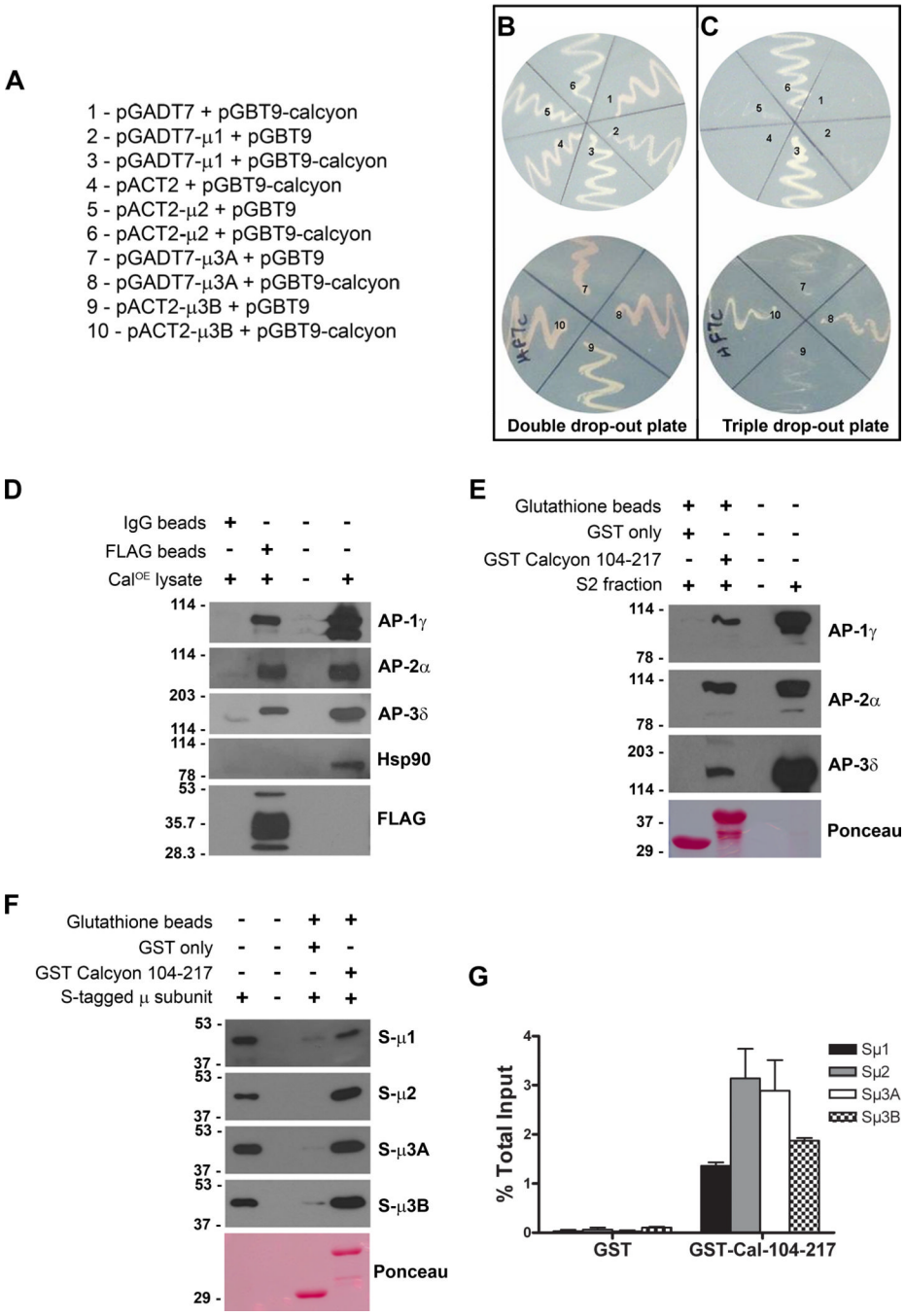

Figure 1. Calcyon directly interacts with 'μ' subunits of adaptor proteins

A. Y2H bait and prey plasmid pairs tested. Plasmid pairs were transformed into HF7C cells, and plated in sectors labeled 'one' to 'ten' on the double (−Leu, −Trp, +His) and triple (−Leu, −Trp, −His) dropout plates shown in B and C, respectively. Growth of colonies co-transfected with pGBT9 calcyon (104–217) and pGADT7-μ1, pACT2-μ2, pGADT7-μ3A or pACT2-μ3B suggests prototrophy on histidine deficient media depends on AP interaction with calcyon. D. Immunoblots of proteins eluted following incubation of Cal^{OE} brain extracts with anti-FLAG or non-immune IgG beads as indicated by the plus and minus signs. Blots were probed with antibodies to γ, α, and δ subunits of AP-1, AP-2, and AP-3, respectively as well as with Hsp90 and FLAG antibodies. E. Immunoblots of proteins eluted

after incubation of control mouse brain S2 fractions with GST or GST-calcyon 104–217 bound to glutathione resin. Blots were probed with antibodies to the γ, α, and δ AP subunits as in D. F. S-HRP detection of AP μ subunits eluted following incubation of resin bound GST or GST-calcyon 104–217 with purified S-tagged μ1, μ2, μ3A and μ3B subunits as indicated to the right of each panel. Ponceau S staining of the lower molecular weight region of the blots in E and F confirms that equivalent amounts of GST and GST-Calcyon 104–217 were used. G. Histogram showing the mean AP μ subunit binding to GST and GST-Calcyon 104–217 detected in three independent experiments expressed as a fraction of input. Error bars indicate the standard error of the mean (SEM).

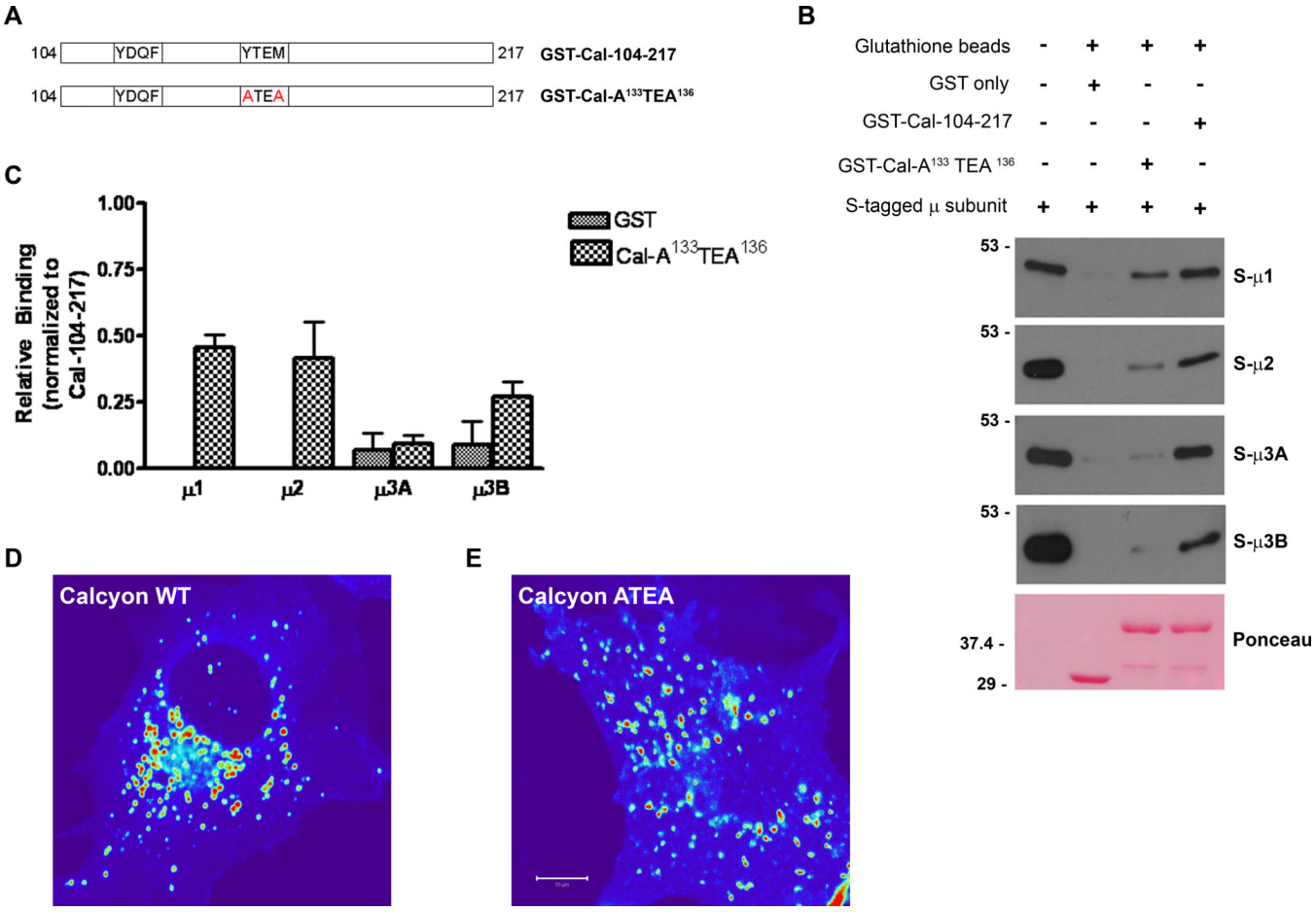

Figure 2. Second 'YXXØ' motif in the calcyon C-terminus is necessary for AP interaction

A. Diagram of GST-calcyon C terminus tyrosine point mutations (shown in red) tested. B. Immunoblots of proteins eluted following incubation of purified S-μ1, S-μ2, S-μ3A and S-μ3B subunit (shown to the right) with the GST-Cal fusion proteins, or GST only as indicated by the plus and minus signs. C. Densitometric analysis of the immunoblots from two independent experiments suggests that the second YXXØ motif of calcyon is necessary for interaction with APs. Bars and error bars in the histogram reflect the mean and SEM. Middle section of confocal z-stack images of Cos-7 cells transfected with (D) mCherry-Calcyon WT and (E) mCherry-Calcyon- $A^{133}TEA^{136}$. The intensity of the mCherry protein fluorescence is displayed using a HeatMap lookup table (bar = 10 mm).

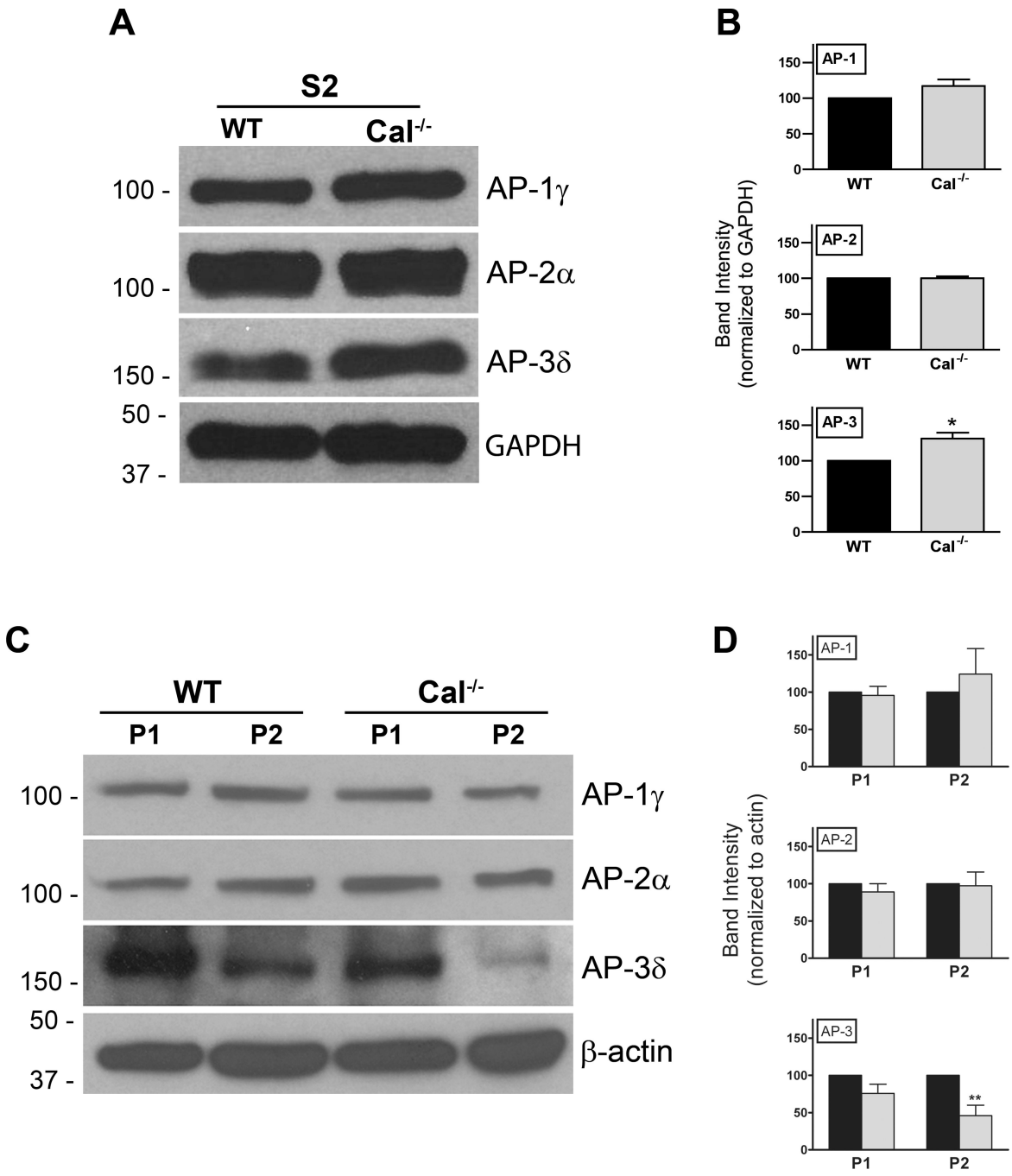

Figure 3. Reduced levels of membrane associated AP-3 in Cal$^{-/-}$ brain

A. Synaptic vesicle containing high-speed supernatants (S2) of WT and Cal$^{-/-}$ brains were separated by SDS PAGE and probed with antibodies to the γ, α, and δ subunits of AP-1, AP-2, and AP-3, respectively, as indicated, as well as with antibodies to GAPDH as a loading control. B. Histogram shows the mean AP levels and error bars indicate SEM detected in the WT (black bars) and Cal$^{-/-}$ brain (grey bars) S2 fractions when normalized to GAPDH levels. AP-3δ is elevated in the Cal$^{-/-}$ S2 fractions compared to levels detected in WT samples (*, $p < 0.05$). C. P1 and P2 membrane fractions of wild type (WT) and Cal$^{-/-}$ brains were separated by SDS PAGE and probed with antibodies to the γ, α, and δ subunits of AP-1, AP-2, and AP-3, respectively, as indicated, as well as with antibodies to β-actin.

Positions of the molecular weight markers are shown to the left. D. Bar graph shows the mean AP levels and error bars the SEM detected in the WT (black bars) and $Cal^{-/-}$ (grey bars) samples following normalization to β-actin levels. $Cal^{-/-}$ values are expressed as percent of WT levels. AP-3δ is reduced in the $Cal^{-/-}$ P2 fractions compared to levels detected in WT samples (**, $p < 0.01$, two-way ANOVA followed by Bonferroni post-test).

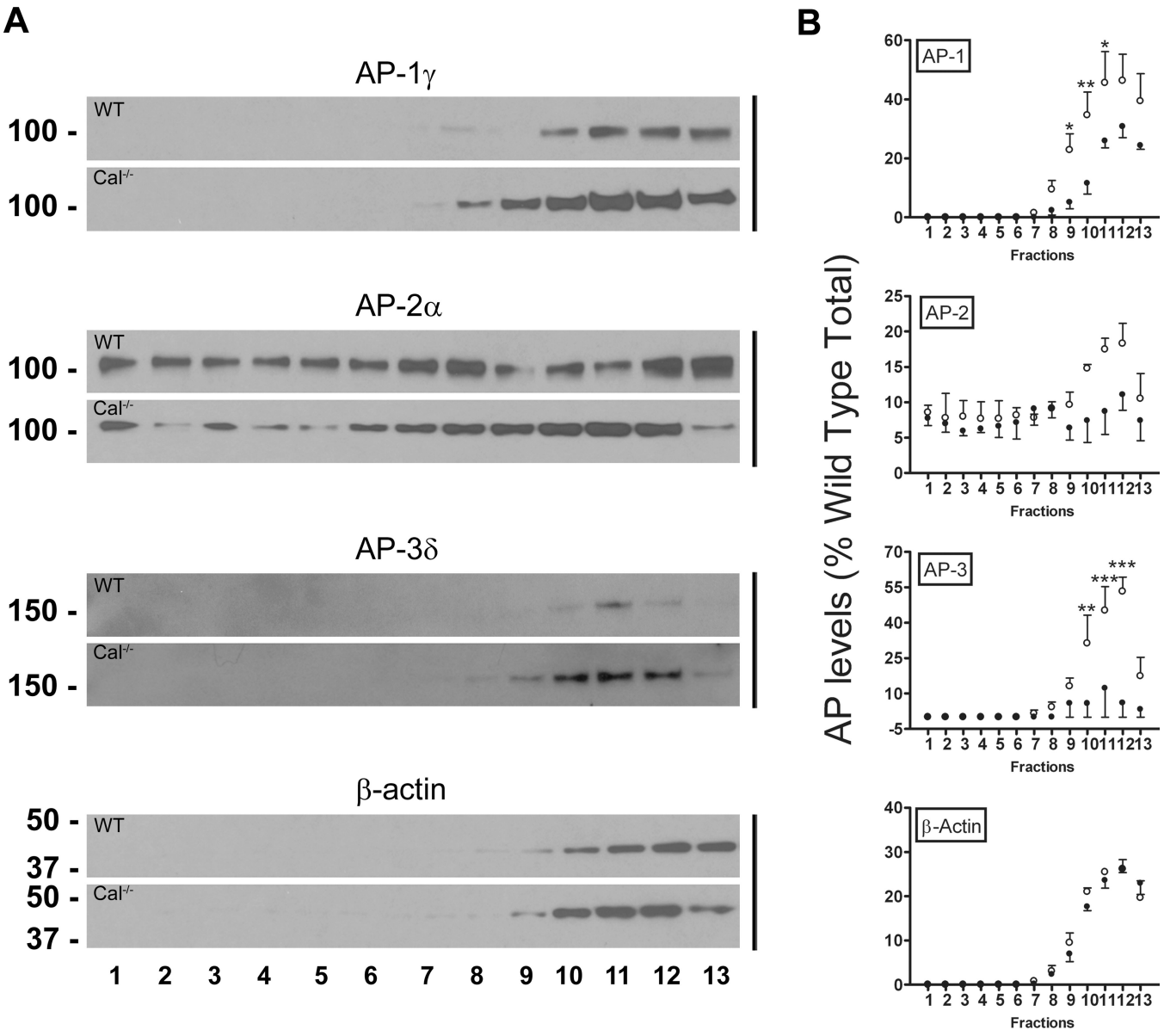

Figure 4. Altered targeting of AP-1 and AP-3 in Cal$^{-/-}$ brain

A. AP levels across the glycerol gradient fractions were determined by re-probing the blots in Fig. S3 with antibodies to the γ, α, and δ subunits of AP-1, AP-2, and AP-3, respectively as well as with β-actin antibodies. B. Sedimentation profile of each protein across the gradient following normalization to the total present in the wild type (WT) sample. Closed and open circles show the mean and error bars, the SEM (n=3) of levels in the WT and Cal$^{-/-}$ fractions, respectively. AP1- γ and AP3- δ levels are increased in the non-SV2 containing fractions (*, ** and***, $p<0.05$, 0.01, and 0.001, respectively, two-way ANOVA followed by Bonferroni post-tests).

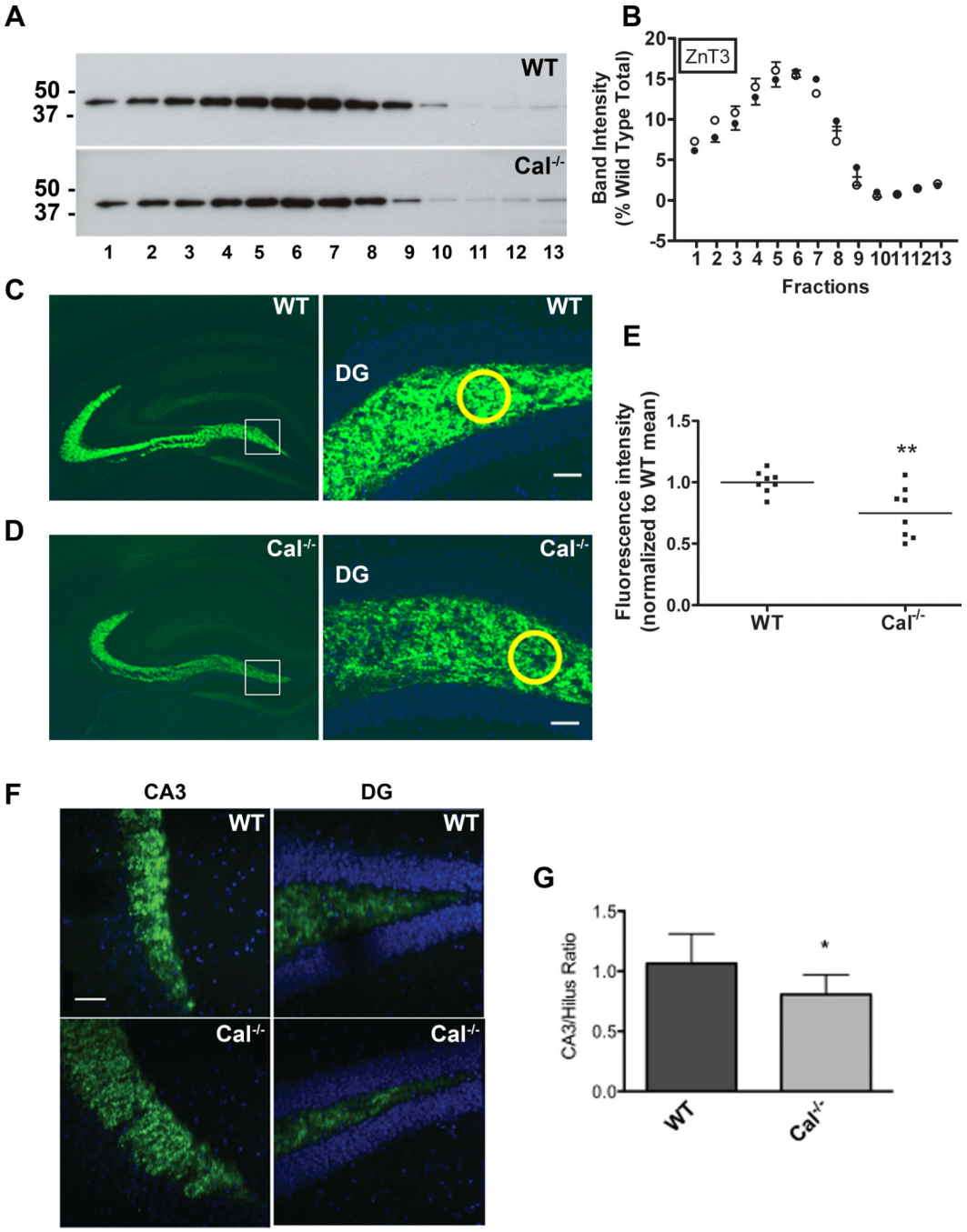

Figure 5. Calcyon regulates trafficking of ZnT3 to mossy fibers

A. Sedimentation profile of ZnT3 in glycerol gradient fractions prepared from wild type (WT) and $Cal^{-/-}$ brains determined by immunoblotting with ZnT3 antibodies. B. Distribution of ZnT3 across the WT (closed circles) and $Cal^{-/-}$ (open circles) gradients following normalization to the total present in the WT gradients. Positions of molecular weight markers are shown to the left. C, D. ZnT3 immunostaining of hippocampal cryosections from WT (C) and $Cal^{-/-}$ (D) mice at low (left) and high (right) magnification. E. Fluorescent staining intensities were obtained in circles (shown in yellow) of equal area positioned over the hilus. Values of ZnT3 staining in $Cal^{-/-}$ samples were normalized to those detected in WT samples in the same rostral-caudal position. Scatter plot shows values

for each sample and horizontal line, the SEM. Compared to levels detected in WT, ZnT3 levels in the hilus of the dentate gyrus are significantly reduced in $Cal^{-/-}$ brain (**, $p<0.01$, t-test). F. Higher magnification (40×) view of ZnT3 staining (green) in mossy fiber terminals in CA3 region (left), and axons in the hilus of the dentate gyrus (right). Nuclei were detected with DAPI (blue). The axon to terminal staining ratio for each sample was determined following measurement of ZnT3 labeling in the hilus and CA3 area using circles of equal size as described above. Bar= 50 μM. G. Histogram with bars and error bars showing the mean CA3/Hilus ratio, and the SEM for the WT and $Cal^{-/-}$ samples. The ratio is significantly reduced in $Cal^{-/-}$ samples suggesting impaired sorting of ZnT3 to terminals in the CA3 (*, $p<0.05$ two-tailed paired t-test).

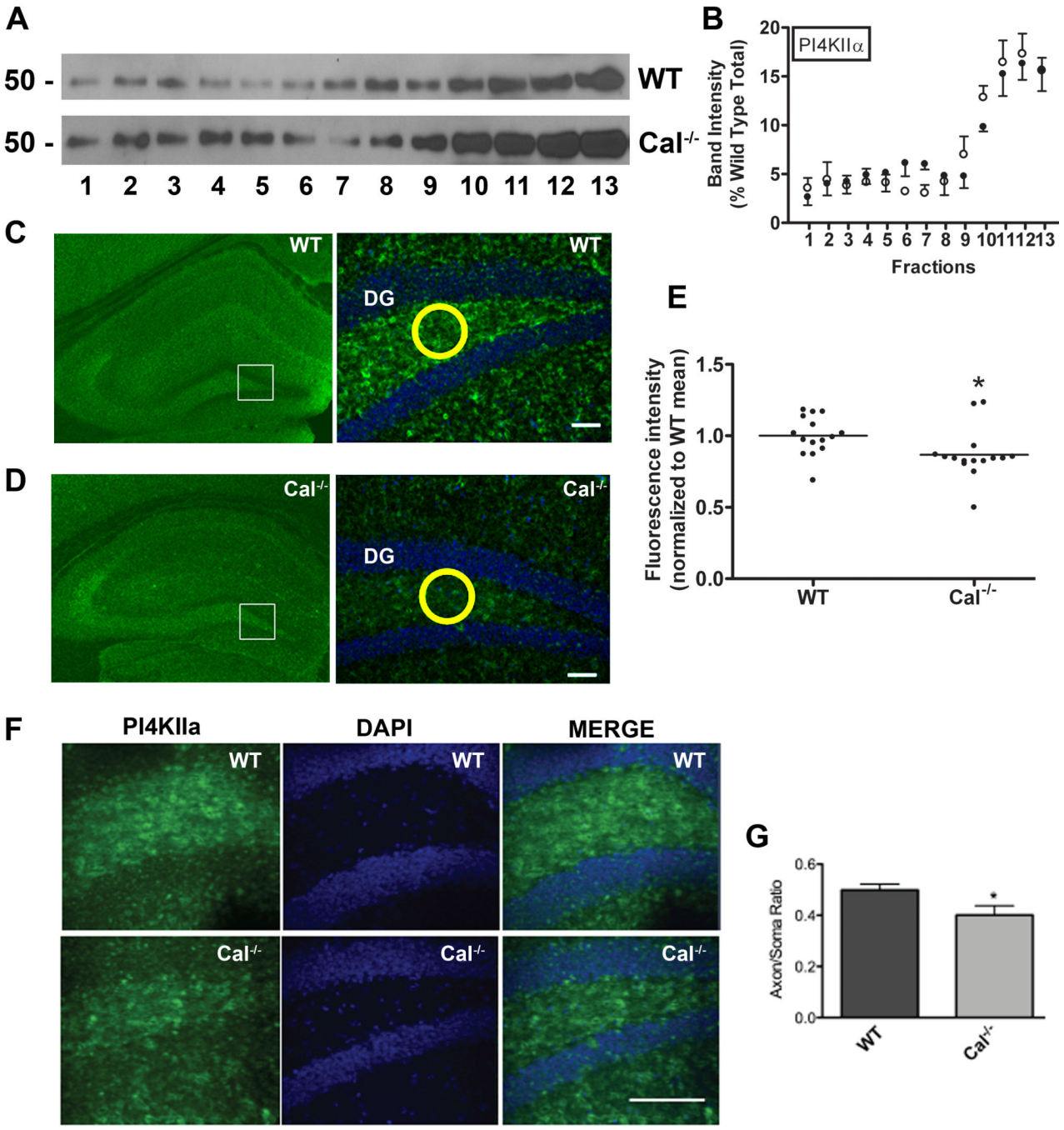

Figure 6. Calcyon regulates expression of PI4KIIα in the hilus of the dentate gyrus

A. Sedimentation profile of PI4KIIα in glycerol gradient fractions prepared from wild type (WT) and $Cal^{-/-}$ brains determined by immunoblotting. B. Distribution of PI4KIIα across the WT (closed circles) and $Cal^{-/-}$ (open circles) gradients following normalization to the total present in the WT samples. Molecular weight markers are shown to the left. C, D. PI4KIIα immunostaining in WT (C),, and $Cal^{-/-}$ (D) hippocampus at low (left) and high (right) magnification. Fluorescent staining intensities were obtained in circles (such as shown in yellow) of equal area positioned over the hilus. Staining in $Cal^{-/-}$ samples was normalized to that detected in WT samples in the same rostral-caudal location. E. Scatter plot showing values for each sample with horizontal line indicating the SEM. Compared to

levels detected in WT, PI4KIIα levels in the hilus of the $Cal^{-/-}$ dentate gyrus are significantly reduced (*, $p<0.05$, t-test). F. Higher magnification (40×) view of PI4KIIα staining of granule cells (green). Nuclei were detected with DAPI (blue). The axon/cell body staining ratio for each sample was determined following measurement of PI4KIIα labeling in the cell body area and adjacent mossy fibers using circles of equal area as described above. Bar= 100 μM G. Histogram with bars and error bars showing the mean axon/soma ratio, and the SEM for the WT and $Cal^{-/-}$ samples (*, $p<0.05$, t-test). The ratio is significantly reduced in $Cal^{-/-}$ samples indicating impaired sorting of PI4KIIα to axons.